Turbulent Heat Transfer in an Internally Heated Fluid Layer

G. Grötzbach

SUMMARY

The method of direct numerical simulation is used to investigate turbulent convection in an internally heated fluid. Two simulations of channels with very different horizontal extensions and different grid widths are analysed. The large scale structures of the flow are completely recorded in the larger channel. The calculated statistical turbulence data of both cases are comparable and even for the smaller channel quite accurate. The reason is found in analyzing a computer generated movie: The macroscopic length scale is kept small by the Rayleigh-Taylor instability.

1. Introduction

The convection in horizontal fluid layers with homogeneous internal heating is a model for certain astrophysical, geophysical, environmental, and technical problems. Similar types of flow occur in the outer layer of some stars, in the earth mantel, in the bioconvection of swimming organisms, in chemical reactors, and in molten fuel of nuclear reactors. In the latter problem the heat transfer was investigated in detail, see [6], the turbulence, however, is investigated rarely, see e.g. the experiments with a heated lower wall [5]. For a channel with quasi infinite horizontal extension and isothermal walls turbulence data have been deduced from direct numerical simulations [2]. The simulations resolved all relevant small scale structures [1], but it remained an open problem whether the horizontal length of the channel was large enough to reproduce adequately the macroscopic scales of the flow.

To solve this problem an additional simulation is presented for a considerably larger channel than in [2]. By comparing both simulations the influence of the horizontal channel width is investigated on some statistical data of turbulence and on the flow structure.

2. Simulation model

The simulation model is the TURBIT-3 code [3]. It is based on the complete three-dimensional time-dependent conservation equations for mass, momentum, and thermal energy. The validity of the Boussinesq approximation is assumed. A finite difference scheme for these equations is deduced

REFINED FLOW MODELLING AND TURBULENCE MEASUREMENTS

Third Int. Symposium on Refined Flow Modelling and Turbulence Measurements, [
July 26 - 28, 1988, Tokyo, □
IAHR-Proc. 1988, pp. 199 - 206□
Publ. Proc.: Refined Flow Modelling and Turbulence Measurements, □
Ed. Y. Iwasa, N. Tamai, A. Wada, Universal Academy Press Inc., Tokyo, □
pp. 267-275, 1989□

by applying Schumann's method [7] to the derivatives in space. This provides equations for surface averaged velocities ${}^{i}\overline{u}_i$ and volume averaged pressure ${}^{v}\overline{p}$ and temperature ${}^{v}\overline{T}$. Integration in time is performed by an explicit Euler-leap frog scheme. The resulting finite difference scheme is discretized on a staggered grid to get exact mass conservation. Subgrid scale terms are neglected as the grids will be chosen to record all relevant flow structures.

For normalization we use the channel height D, time D/u_o, velocity $u_o = (g\beta\Delta T_o D)^{1/2}$, and temperature $\Delta T_o = \langle T_{max} - T_w \rangle$. The latter is calculated using the relation between Damköhler and Nusselt numbers at the lower and upper wall, Nu_1 and Nu_2: $Da_o = QD^2/(\lambda\Delta T_o) = Nu_1 + Nu_2$, with Q = volumetric heat source and λ = thermal conductivity. The Prandtl number is Pr = v/a with v = viscous diffusivity and a = thermal diffusivity, the Rayleigh number is $Ra = g\,\beta\,Q\,D^5/(va\lambda)$ with g = gravity and β = volume expansion coefficient.

3. Case specifications

The convection of an internally heated fluid bounded by two horizontal rigid walls is considered. In both horizontal directions periodicity is assumed with periodicity lenghts X_i, Table 1. In the new simulation, case 12, X_i is more than twice the value as used in case 11 taken from [1,2,3] and more than four times the wavelength of the flow pattern observed at onset of convection. As the wavelength is expected to decrease with increasing Ra at this type of flow, case 12 should show no deficiencies due to too short a periodicity length. In the vertical direction the velocities are set to zero at the walls, and the wall shear stresses and wall heat fluxes are approximated by linear finite difference approximations. The wall temperatures T_w are set equal and kept constant in space and time.

Table 1: Case specifications and time intervals (i = 1, 2)

Case	N_i	N_3	X_i	Δx_i	Δx_{3w2}	N_t	t_{max}	t_{CPU}	N_{tav}	Δt_{av}
11	64	32	2.8	.04375	.020	4,040	40.2	1.5 h	15	5.6
12	180	32	7.2	.04	.005	101,920	88.7	223.1 h	17	20.8

The numbers N_i of nodes chosen result in the finer horizontal grid widths $\Delta x_{1,2}$ for case 12; the vertical distribution of the non-equidistant grid width Δx_3 of case 11 is slightly rearranged to have a much finer resolution near the upper wall w2 in case 12, Table 1. The Prandtl number is six, the Rayleigh number is $107 \cdot Ra_c = 4 \cdot 10^6$.

The simulations are started from zero velocity and from approximated vertical temperature profiles on which random fluctuations are superposed. The initial ΔT_o is calculated by means of correlations given in [4] which results in $Da_o = 15.7$. The simulations are stopped after N_t time steps at time t_{max} when the Nusselt numbers at both walls (Fig. 1) and the mean value of the turbulence energy in the channel analysed from the time-dependent results oscillate around mean values, this means when fully developed flow is simulated for a certain time. The computing times t_{CPU} are given in equivalent hours for the current code version with improved vectorization and a SIEMENS/FUJITSU VP50 vector computer with a storage of 64 MBytes, Tab. 1.

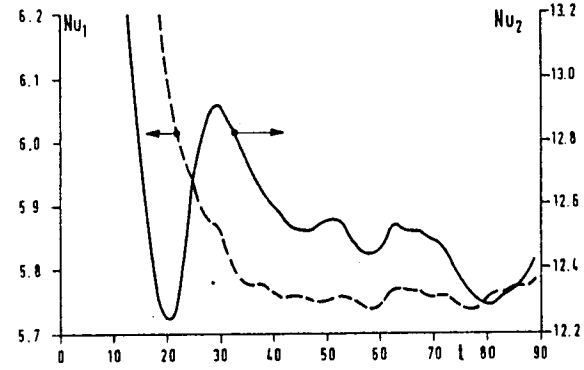

Fig. 1: Time-dependent horizontally averaged Nusselt numbers at both walls for case 12.

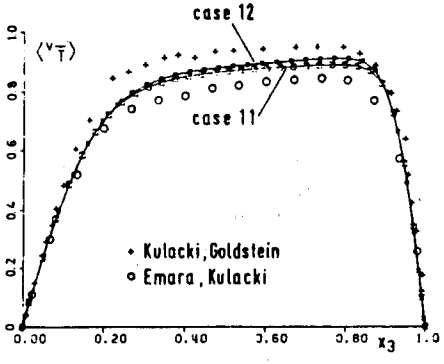

Fig. 2: Vertical time mean temperature profiles. The published data are taken from [6].

4. Simulation Results

The complete three-dimensional results for the three velocity components, pressure, and temperature are stored for a certain number of time steps. To obtain reasonable statistical data from the time dependent results, averages $\langle y \rangle$ are formed for a calculated variable y over horizontal planes, and these are averaged over $N_{t\,av}$ time steps distributed within the period Δt_{av} at the end of the simulated problem time, see Table 1. The tremendous increase in Δt_{av} from case 11 to 12 reduces the statistical coupling in time, compare Fig. 1, and that of X_i the coupling in space.

4.1 Verification

The Nusselt numbers calculated at both walls for case 11 are in the middle of the scatter band of experimental data [1,6], and those calculated for case 12 agree as well. Fig. 1 shows that the Nusselt numbers, determined by horizontal averaging only, achieve deviations from the mean value below ±2.5% even after less than half the problem time.

The calculated vertical time mean temperature profiles are compared to the experimental data from Kulacki and to the two-dimensional calculation by Emara [6] in Fig. 2. Both simulations differ by 3.5% from one another. The reason might be that the time t_{max} simulated with the coarser grid is too small to really get fully developed flow, see Table 1 and Fig. 1. In the boundary layers both simulations agree as well with the experimental data

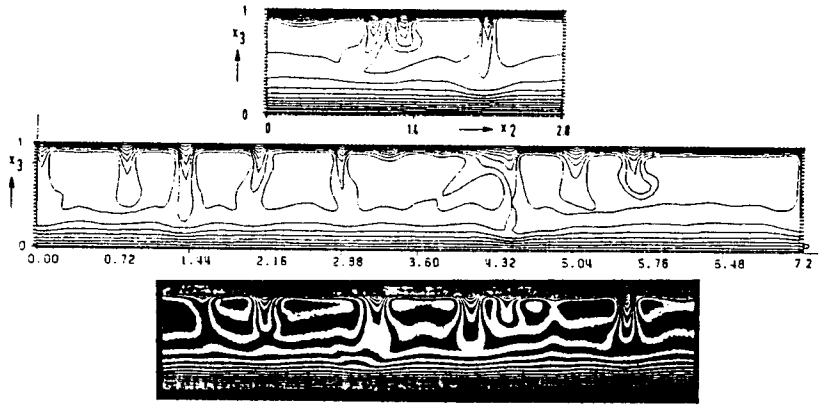

Fig. 3: Vertical cuts of calculated temperature fields at any time and interferograms from experiments by Jahn. The contourline increment is $\Delta = 0.08$ for case 11 and 0.125 for case 12.

as the Nusselt numbers do. In the region $0.3 < x_3 < 0.8$ a somewhat larger increase in temperature is predicted by both models than in the experiment.

The local convection phenomena are compared to experiments by cuts through the temperature field. In the vertical cuts one finds the internally heated hotter fluid bounded by the colder walls, Fig. 3. The lower boundary layer is stably stratified. The core is weakly stable. The upper boundary layer is unstable and therefore drives the flow. Here cold plumes develop, fall, and some of them deeply penetrate into the lower layer. Both simulations reproduce the structures of the plumes as observed in the experiments [4]. All three results give about the same vertical temperature distribution. Thus, the predicted temperature increase in Fig. 2, is verified by this experiment.

Horizontal cuts are given for a plane near the temperature maximum T_{max} in Fig. 4. Most of the cold plumes form cells around a hot isothermal core. The cells are connected randomly. Some smaller plumes occur in larger cells. Again, the structures simulated are comparable to and agree with those in the experiment [4].

So far the simulation results are compared to all types of directly recorded experimental data available for this flow at the parameters considered, and no problem with the smaller periodicity length becomes obvious.

4.2 Predicted turbulence data

In this chapter the influence of the periodicity lengths on the predicted turbulence data is investigated.

The root-mean-square (rms) values for the velocity fluctuations show that in the inner part of the channel most energy is in the vertical component, Fig. 5. The horizontal components are more important only within the boundary layers. The data for both horizontal components of case 12 roughly coincide whereas the result for the smaller channel shows statistical errors due to insufficient averaging. This deviation is completely associated with the component i = 2 in case 11; all other curves coincide nearly totally.

The pressure strain terms, which are also called the tendency-toward-isotropy terms, show near midplane minor energy transfer from the vertical to the horizontal velocity fluctuations, Fig. 6. This indicates that the down-

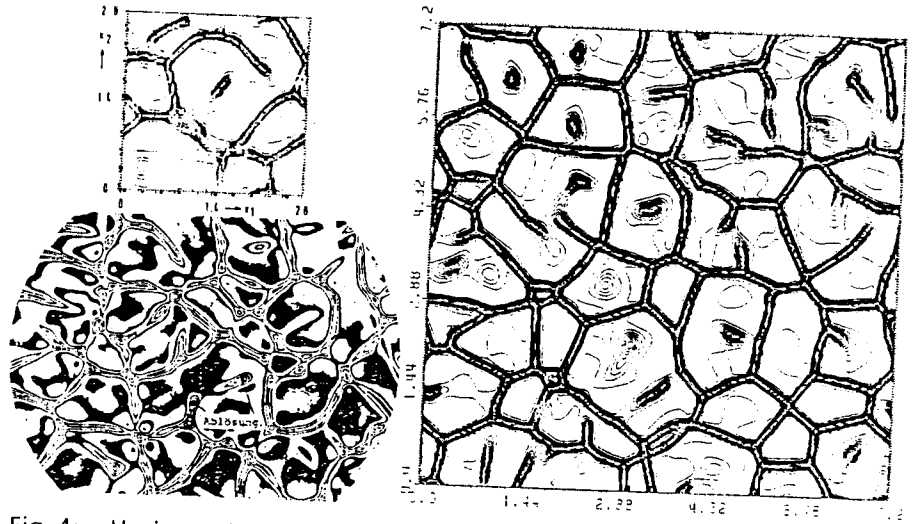

Fig. 4: Horizontal cuts of calculated temperature fields at any time and interferograms from experiments by Jahn. $\Delta = 0.0625$

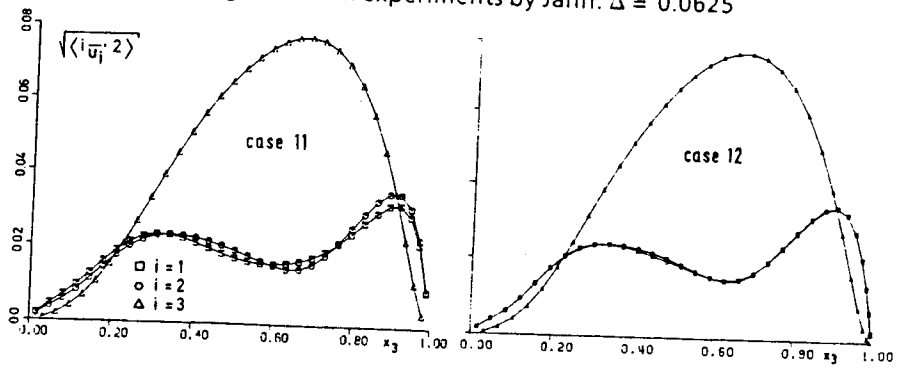

Fig. 5: Calculated rms-values of the velocity fluctuations

flowing plumes interact weakly with the ambient slowly upflowing fluid. Near the upper wall, where less energy is in the vertical than in the horizontal components (Fig. 5), these terms show considerable energy transfer from the vertical to the horizontal components. On this way part of the energy directly produced by the buoyancy term in the vertical component is redistributed to the horizontal ones and energy is transported from a lower to a higher level. This feature is consistently given by both simulations.

The calculated rms-values of temperature fluctuations show a small relative maximum in the stable layer, Fig. 7. In this region most of the downcoming plumes come to rest. The absolute maximum is in the unstable layer, slightly above the position of the temperature maximum. Except at the lower maximum both results agree.

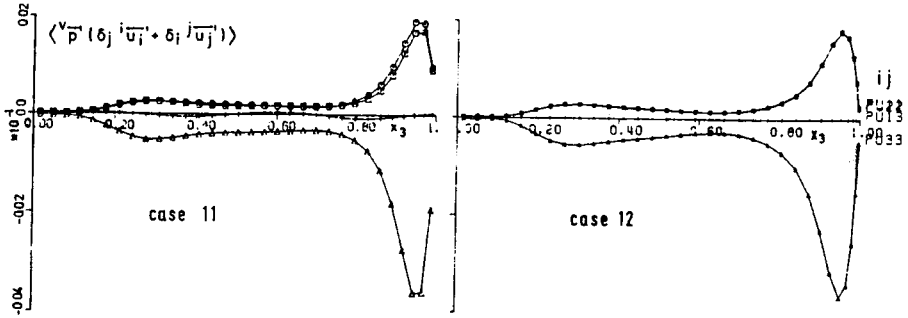

Fig. 6: Calculated pressure strain terms

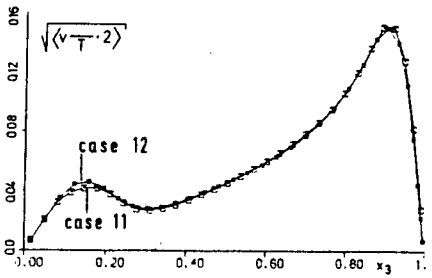

Fig. 7: Calculated rms-values of temperature fluctuations

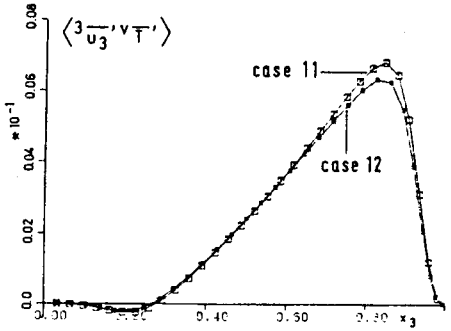

Fig. 8: Calculated vertical turbulent heat flux

The turbulent heat flux in the vertical direction is calculated to be negative in the lower, mainly conduction controlled, boundary layer, Fig. 8. In the upper three quarters of the channel the flux is directed upwards. As the temperature maximum is at $x_3 \approx 0.77$ we find an extensive region with countergradient turbulent heat flux. This phenomenon is discussed in [2,3], and reasons are given in [8]. Both simulations agree except at the maximum. Since the vertical velocity and temperature fluctuations of both cases do not differ the difference in the turbulent heat flux can only be due to a not fully developed flow or insufficient averaging of case 11.

4.3 Macroscopic length scale

Two-point correlations $R_{ii}(x_1) = \langle u'_i(x)\, u'_i(x + x_1)\rangle / \langle u'_i(x)\, u'_i(x)\rangle$ are calculated from the velocity fluctuations slightly above midplane, Fig. 9. The rapid decrease at small displacements is identical in both simulations. At $x_1 > 0.3$ case 12 gives a somewhat flatter decrease for R_{22} than case 11. The zero crossings for u_1 and u_3 in both cases occur at about the same position; this means the typical wavelength λ of the large scale structures is roughly the same in both simulations. With $\lambda \cong 0.6$ it is much smaller than $\lambda_c = \pi/2$ at onset of convection. The strong oscillations and non-zero values at $x_1 > 0.8$ in case 11 show that the smaller periodicity length causes statistical spatial coupling which cannot be detected in Fig. 4. The other simulation is clearly free of this problem.

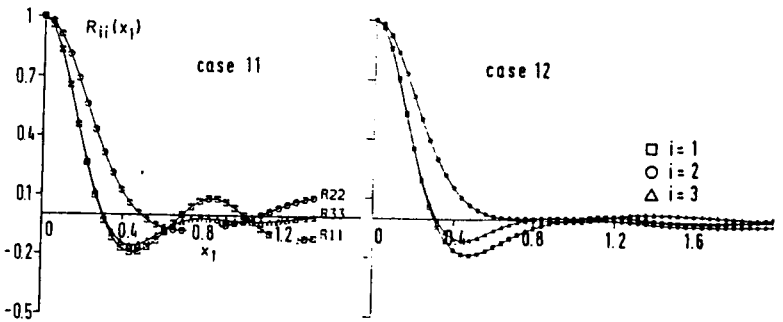

Fig. 9: Two-point velocity auto-correlations in x_1 direction at $x_3 = 0.504$ (case 11) and $x_3 = 0.554$ (case 12).

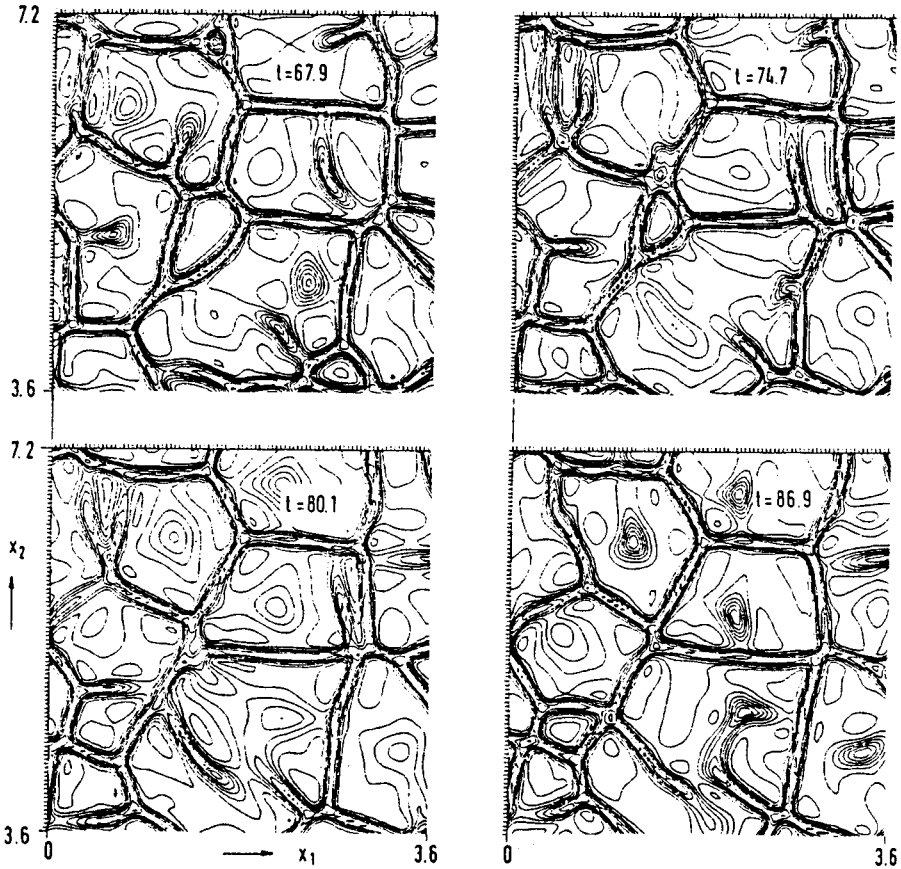

Fig. 10: Time-dependent horizontal quarter sections through the temperature field; case 12, $\Delta = 0.0625$, $x_3 = 0.953$.

The meaning of the length scale deduced from R_{ii} is investigated on the basis of a movie which presents calculated time-dependent flow structures within the upper boundary layer, Fig. 10. Some smaller open or closed cells contract to knots and widen the neighbouring cells. Mainly in the larger cells round plumes develop, grow to plane plumes, merge with other ones, and form new cells. The range of wavelengths λ_{max} covered by the cells is between zero and about 1.7. The plumes developing within cells reduce the wavelength to 0.5 to 0.8. This is in accordance with the value estimated from R_{ii} and also with $\lambda = 0.7$ determined from the energy spectra for case 11 [3]. As in fact in all larger cells plumes develop which reduce the length-scale one might deduce the wavelength found is about the critical one for the Rayleigh-Taylor instability of the upper boundary layer.

5. Conclusions

Both simulations with differing small scale resolution and very different horizontal extension could be verified by all types of experimental data published for this type of flow. The results confirm that the requirements [1] to resolve the relevant small scales are sufficient for calculation of the turbulence data considered here. In these data both simulations differ only slightly due to insufficient averaging in the analysis of the older simulation with the smaller periodicity length. Nevertheless, both simulations can be used as a data base to analyse any turbulence data, but the new one will be more suited for data mainly determined by large scale structures.

The new simulation also confirms that the macroscopic length scale of this flow decreases with increasing Rayleigh number. The movie shows that the Rayleigh-Taylor instability keeps the always growing length scale small. From this and from the analysed two-point correlations it follows that in future simulations the periodicity lengths need not to exceed the $2 \cdot \lambda_{max}$ observed visually or the 4 to $5 \cdot \lambda$ calculated. This allows to perform accurate studies for similar Rayleigh numbers by means of direct numerical simulations with grids somewhat larger than the coarser one used here. With the node numbers of the larger grid highly turbulent flows can be investigated on present day computer systems up to about 10^4 times the critical Rayleigh number. Thus, the method of direct numerical simulation may be used for parameter ranges which were only covered by experiments, if any.

6. Acknowledgements

Sincere thanks go to Doug Reeder, UCSB, Santa Barbara, Cal., who helped to vectorize the TURBIT code and to Wolfgang Olbrich, KfK/IRE, who developed the software for the movie and produced it. Support by members of the KfK computer centre during implementation and calculation on the VP50 is also gratefully acknowledged.

7. References

1. Grötzbach, G. (1981), Spatial resolution requirements for numerical simulation of internally heated fluid layers, in Numerical Methods in Laminar and Turbulent Flow, Ed. C. Taylor, Pineridge Press, p. 593-604.
2. Grötzbach, G. (1982), Direct numerical simulation of the turbulent momentum and heat transfer in an internally heated fluid layer, in Heat Transfer 1982, Ed. U. Grigull et al., Hemisphere, Vol. 2, pp. 141-146.
3. Grötzbach, G. (1987), Direct numerical and large eddy simulation of turbulent channel flows, in Encyclopedia of Fluid Mechanics, Ed. N.P. Cheremisinoff, Gulf Publ., Vol. 6, pp. 1337-1391.

4. Jahn, M. (1975), Holographische Untersuchung der freien Konvektion in einer Kernschmelze, Dissertation, TU Hannover.
5. Kikuchi, Y., Shioyama, T., Kawara Z. (1986), Turbulent heat transport in a horizontal fluid layer heated internally and from below, Int. J. Heat & Mass Transfer 29, p. 451-461.
6. Kulacki, F.A. and Richards D.E. (1985), Natural convection in plane layers and cavities with volumetric energy sources, in Natural Convection, Ed.: S. Kakac et al., Hemisphere, pp. 179-255.
7. Schumann, U. (1975), Subgrid scale model for finite difference simulations of turbulent flows in plane channels and annuli, J. Comp. Phys. 18, p. 376-404.
8. Schumann, U. (1987), The countergradient heat flux in turbulent stratified flows, Nucl. Engng. & Design 100, p. 255-262.

Y. IWASA
N. TAMAI
A. WADA

EFINED FLOW MODELLING AND TURBULENCE MEASUREMENTS

oceedings of the Third International Symposium on
lined Flow Modelling and Turbulence Measurements
d on 26–28 July, 1988 in Tokyo, Japan

ited by Y. Iwasa, *Kyoto University*
N. Tamai, *University of Tokyo*
A. Wada, *Tokai University*

This book presents a selected collection of the lectures and papers presented at the Third ernational Symposium on Refined Flow Modelling and Turbulence Measurements held in kyo, Japan on July 26–28, 1988.

The utilization of high-speed, large-capacity computers has contributed much to the provement of accuracy in numerical models of fluid phenomena in the fields of nuclear wer, energy, environment, construction, geophysics, etc. On the other hand, highly dvanced modelling of flow is now possible thanks to greater progress in the measurement of ws, and particularly in the techniques of turbulence measurement. Specifically, the perimental data to validate computations are very important as input to the numerical odelling, and they are of deep significance to discussions of effects which are not yet covered numerical models. The objective of the Symposium is to bring together scientists and gineers, working in the fields mentioned above, to discuss the latest advances in flow odelling and in turbulence measurements.

The lectures and papers selected have been re-edited into twelve parts including keynote ctures delivered by Professors W. Rodi, W. Z. Sadeh and M. Akiyama, which highlighted the ate-of-the-art in the computational fluid dynamics, experimental fluid dynamics and pplications.

Topics of papers gathered in this book range from modelling in turbulent flows and heat ansfer, progress in numerical techniques, dispersion, stratified flow in atmosphere and water nvironments to flows in rivers and open channels.

SBN 4-946443-03-7

Universal Academy

Refined Flow Modelling and Turbulence Measurements

Refined Flow Modellin
and
Turbulence Measuremer

Edited by
Y. IWASA
N. TAMAI
A. WADA

Universal Academy Press, Inc.

Tokyo 1989

pp. 267-275

Universal Academy Press, Inc.